NASA TM-87682

NASA Technical Memorandum 87682

DIVERGENCE STUDY OF A HIGH-ASPECT RATIO, FORWARD-SWEPT WING

STANLEY R. COLE

JUNE 1986

NASA

National Aeronautics and
Space Administration

Langley Research Center
Hampton, Virginia 23665

NF01259

DIVERGENCE STUDY OF A HIGH-ASPECT RATIO, FORWARD-SWEPT WING

Stanley R. Cole
NASA Langley Research Center
Hampton, VA 23665-5225

ABSTRACT

An experimental wind-tunnel study to determine the divergence characteristics of a high-aspect ratio, forward-swept wing has been conducted in the NASA Langley Research Center (LaRC) Transonic Dynamics Tunnel (TDT). The rectangular wing used for this study had a panel aspect ratio of 9.16 ($\Lambda = 0°$) and the sweep angle could be set at $\Lambda = 0°$, $-15°$, $-30°$, $-45°$, or $-60°$. A rectangular wing tip shape was tested at each of these sweep angles. In addition, a tip shape parallel to the freestream flow was tested for a wing sweep angle of $\Lambda = -45°$. The root of the wing was cantilever mounted to the wall of the wind tunnel. Divergence conditions were measured at $M = 0.4$ for each sweep angle and tip configuration tested. Subcritical response techniques were used to extrapolate to the divergence conditions during the wind-tunnel test. The primary objective of this test was to obtain data which could be used to verify for this configuration the divergence prediction capability of an aeroelastic analysis code. Subsonic lifting surface theory (kernel function) aerodynamics are utilized by this particular code. The analytical predictions of divergence were found to be significantly conservative at all forward sweep angles. At $\Lambda = -45°$, the analysis was 14 percent conservative. The effect of the two tip shapes on the divergence dynamic pressure was predicted accurately by the analysis. The divergence condition for the tip shape parallel to the flow occurred at a dynamic pressure 14 percent higher than the divergence condition with a rectangular tip shape.

NOMENCLATURE

AR	aspect ratio
EI	bending stiffness, $lb \cdot ft^2$
f	frequency, Hz
g	incremental damping
GJ	torsional stiffness, $lb \cdot ft^2$
M	Mach number
M_e	moment about elastic axis, $ft \cdot lb$
q	dynamic pressure, lb/ft^2
q_D	divergence dynamic pressure predicted by a subcritical response technique, lb/ft^2
q_{ref}	reference dynamic pressure, lb/ft^2
V	velocity, ft/sec
y	spanwise distance along elastic axis from wing root, ft
α	root angle of attack, deg
Δ	divergence index parameter $= 1-(q/q_D)$
λ	slope of M_e-versus-α curve, $ft \cdot lb/deg$
Λ	mid-chord sweep angle, deg
ρ	density, $lb \cdot sec^2/ft^4$

Subscripts

a	analysis result
n	nth value
r	rth value
45	forward sweep angle, deg

INTRODUCTION

The combination of vertical take-off and high-speed flight is a desirable feature for many aircraft applications. The X-Wing concept[1] vehicle, currently under examination in a joint NASA/DARPA flight test demonstration program, is an excellent example of a vehicle which has both of these capabilities. The X-Wing achieves these features by flying in either a helicopter or a fixed-wing mode. The "conversion" from one configuration to the other takes place during flight by stopping/starting the four-bladed rotor. In the fixed wing configuration, the blades (or wings in this instance) are oriented at $\Lambda = +45°$ and $\Lambda = -45°$. Therefore, two of the rotor blades are actually high-aspect ratio, forward-swept wings. The scope of the current flight test program is to demonstrate the conversion phase of flight. The Rotor System Research Aircraft (RSRA)[2] will be utilized to achieve this first step toward a successful X-Wing vehicle.

The present study was conducted to obtain data which could be used to verify the prediction capabilities of a currently available aeroelastic analysis code for this unusual configuration (high-aspect ratio, forward-swept wing). An experiment was conducted in the NASA Langley Transonic Dynamics Tunnel (TDT) on a previously existing model with an aspect ratio similar to that of the RSRA/X-Wing rotor blade. This model had a panel aspect ratio of 9.16 (unswept) compared to the RSRA/X-Wing design value of 9.61 (see Fig. 1). Aeroelastic analyses were conducted for each condition tested in the TDT for this comparison. The wind-tunnel model was tested at various forward sweep angles to determine the effect of other azimuth angles which rotor blades on a X-Wing vehicle would encounter during the conversion phase of flight. A rectangular tip shape (as currently planned for the RSRA/X-Wing vehicle) was used during most of the experiment. A tip parallel to the flow in the $\Lambda = -45°$ position was also tested for further correlation with analysis. General aeroelastic characteristics of the high-aspect ratio, highly swept wing and the prediction capabilities of the analysis code are discussed in this report.

TEST APPARATUS AND PROCEDURES

Wind-Tunnel Model

The model used in this study was untapered, had a 4.51 ft semi-span, and had a semi-span aspect ratio of 9.16 in the unswept position as
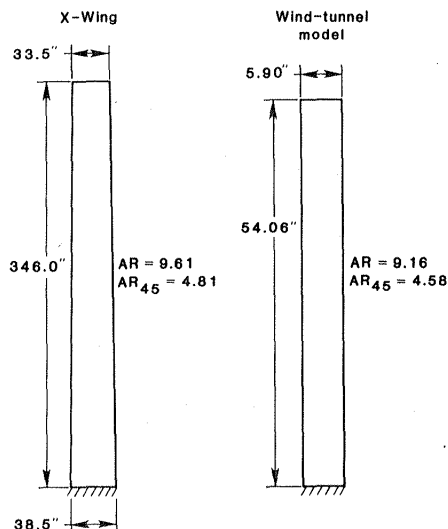
Fig. 1.- Comparison of planform geometry of the
X-Wing flight configuration and the
wind-tunnel model.

shown in Fig. 1. The airfoil section was a NACA
0014. The model wing was constructed of a
layered fiberglass shell, which provided both
structural stiffness and the airfoil shape, with
a rectangular aluminum spar located at the 30
percent chord position to increase the bending
stiffness. This construction, and the airfoil
shape, are illustrated in Fig. 2. Semicircular
wing tips made of balsa wood were used to
improve the flow over what otherwise would have
been a blunt wing tip in the forward-sweep
positions.

A splitter plate was mounted to the support
system at the wing root to provide a reflection
plane for the model. Fig. 3 is a photograph of
the model mounted in the tunnel in the $\Lambda = -45°$
position. The model was clamped in a canti-
levered manner to the support system which was
clamped to the wind-tunnel sidewall turntable.
This allowed the angle of attack to be changed
during testing.

The wing was positioned manually to sweep
angles of $0°$, $-15°$, $-30°$, $-45°$, or $-60°$. A
composite photograph showing the model in the
various sweep positions is shown in Fig. 4. The
model was tested with a rectangular wing tip at
each azimuth angle as shown in the figure. In
addition, the wing tip was modified such that
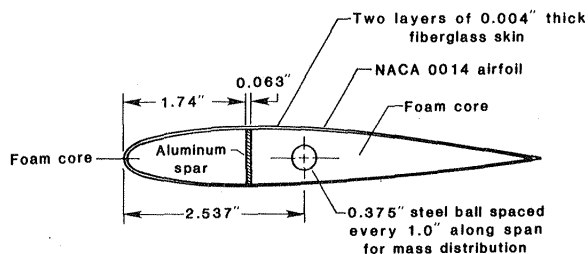the tip was parallel to the freestream flow when

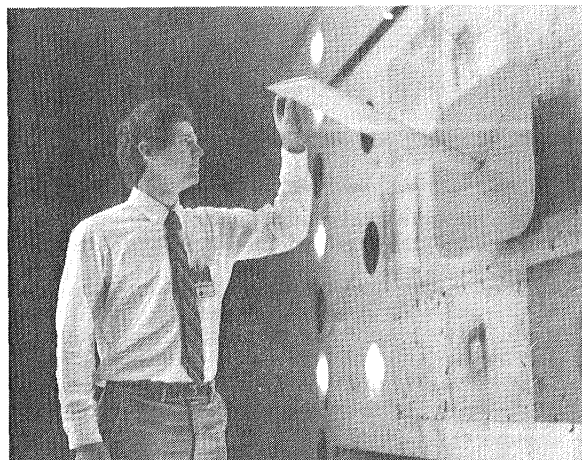Fig. 2.- Cross-section view of model
construction.
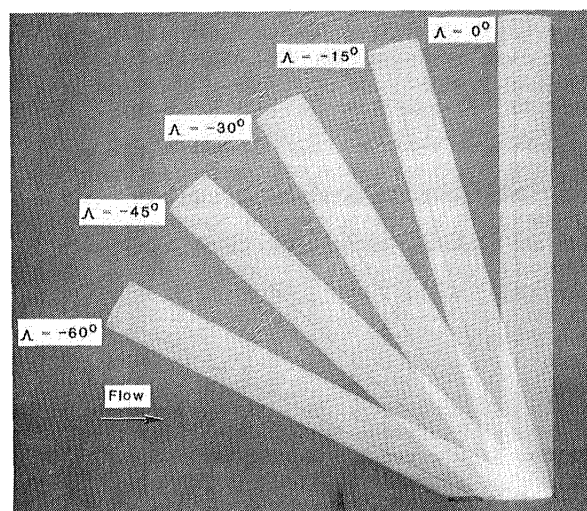

Fig. 3.- Model mounted in the TDT, $\Lambda = -45°$.

Fig. 4.- Composite photograph showing each sweep
angle tested.

tested in the $\Lambda = -45°$ position. Sketches of
the two tip shapes are shown in Fig. 5.

Vibration and stiffness characteristics of
the wind-tunnel model were measured. Natural
frequencies were measured from the output of
electrical resistance strain-gage bridges which
were mounted near the wing root and oriented
such that bending and torsional strains were
measured. Measured and calculated natural
vibration frequencies are given in Table 1.

Wind Tunnel

The model tests were conducted in the
Langley TDT[3]. The TDT is a continuous-flow wind
tunnel capable of subsonic and transonic
speeds. The test section of the tunnel is 16.0
ft square with cropped corners. The TDT can use
either air or Freon* 12 as the test medium.

*Freon: Registered trademark of E. I. duPont de
Nemours & Co., Inc.

2

Table 1· Natural vibration frequencies of the wind-tunnel model.

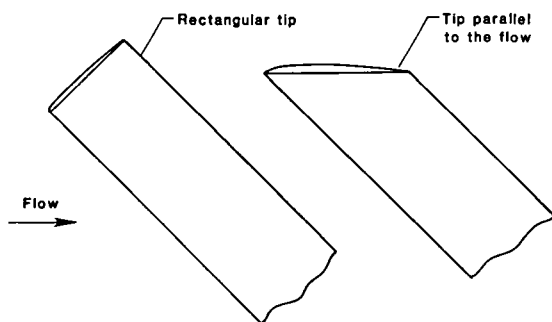| Mode	Calculated f, Hz	Measured f, Hz
1-First bending	5.4	5.3
2-First chordwise bending	22.0	23.8
3-Second bending	33.6	33.0
4-First torsion	62.5	71.3
5-Third bending	92.3	89.5

Fig. 5 - Tip shapes tested in the Λ = -45° configuration.

Freon 12 was used for the present study. A Mach number range from near zero to 1.2 and a pressure range from near zero to atmospheric pressure are available.

Test Procedures

Experimental predictions of static aeroelastic divergence were made using subcritical response techniques[4]. For each sweep angle tested, subcritical data were taken at gradually increasing values of dynamic pressure At each dynamic pressure the model angle of attack was first adjusted to a 1-g lift condition so that the weight of the model was aerodynamically supported. The angle of attack was then incrementally increased and the root bending moment was measured at each angle of attack. These data were used to predict the dynamic pressure at which divergence would occur.

Two subcritical response techniques, an improved static Southwell method and the divergence index method, were used during this test. Reference 4 discusses these prediction methods in greater detail. The improved static Southwell method uses all of the angle of attack data obtained at each dynamic pressure tested (Fig. 6). The slope, λ, of the M_B-versus-α data is plotted against λ/α for each dynamic

pressure (Fig. 7). The slope of a linear fit of the resulting plot is the predicted divergence dynamic pressure.

The divergence index method also uses all of the angle of attack data obtained at each dynamic pressure to calculate λ. The divergence index parameter,

$$\Delta_n = \frac{1 - (q_n/q_r)}{1 - (\lambda_n/\lambda_r)},$$

is then calculated. The subscript r indicates a reference condition, which for this test was the lowest dynamic pressure data set obtained at each sweep angle. Using the divergence index method, Δ is plotted versus q (Fig 8) and a linear fit is imposed on the experimental results such that Δ is related to q as follows

$$\Delta = 1 - \frac{q}{q_D}$$
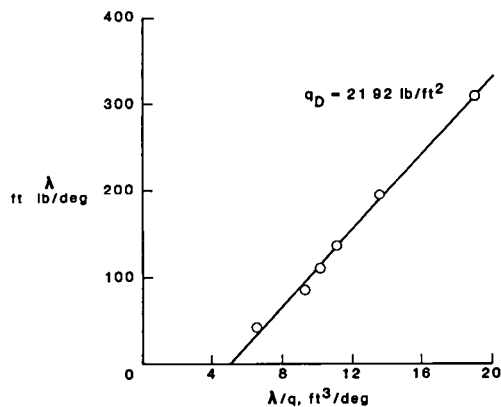
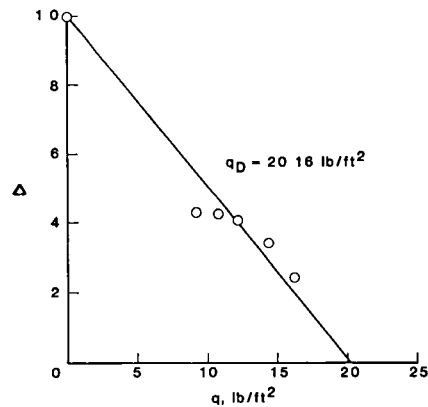Therefore, at a dynamic pressure of zero, the

(a) Λ = -45°, M = 0.4
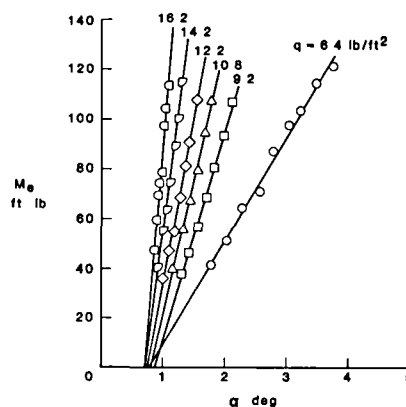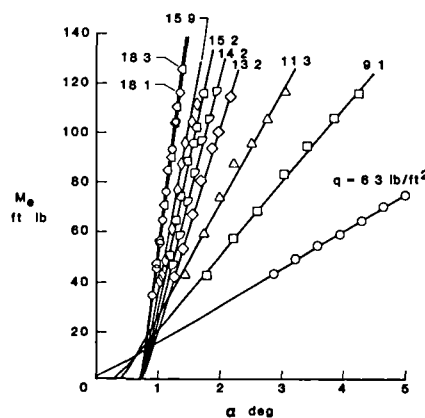
(b) Λ = -60°, M = 0.4

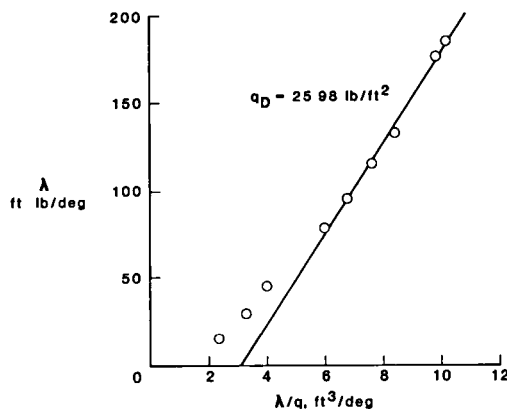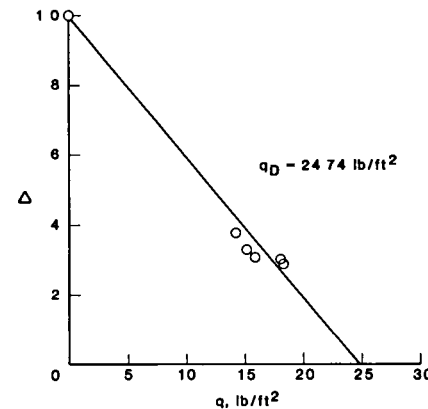Fig 6.- Typical data obtained for subcritical response divergence predictions.

3

$q_D = 21\ 92\ lb/ft^2$

Λ
ft lb/deg

Λ/q, ft^3/deg

(a) $\Lambda = -45°$, M = 0.4

$q_D = 20\ 16\ lb/ft^2$

Δ

q, lb/ft^2

(a) $\Lambda = -45°$, M = 0.4

$q_D = 25\ 98\ lb/ft^2$

Λ
ft lb/deg

Λ/q, ft^3/deg

(b) $\Lambda = -60°$, M = 0.4

Fig. 7.- Typical results of the Southwell method divergence prediction technique.

$q_D = 24\ 74\ lb/ft^2$

Δ

q, lb/ft^2

(b) $\Lambda = -60°$, M = 0.4

Fig. 8.- Typical results of the divergence index method prediction technique.

divergence index parameter equals one Further, at $\Delta = 0$ the straight line extrapolation intercepts the predicted divergence dynamic pressure.

ANALYTICAL TOOLS

Aeroelastic analyses were conducted for the wind-tunnel model to determine the validity of the analysis code for a high-aspect ratio, highly-swept wing. A vibration analysis was performed with the finite element method program[5] Engineering Analysis Language (EAL). General beam elements were utilized to assemble the finite element model. The beam element simulation for the EAL analysis is shown in Fig. 9. Elements were arranged to simulate the stiffness properties along the measured elastic axis of the model. Constant stiffness properties derived from laboratory measurements

were used for the beam elements. The measured stiffness properties and the constant property values used in the finite element model are shown in Fig. 10. Lumped masses were located to simulate the chordwise center of gravity position of the model. These lumped masses were offset from the structural elastic axis by very stiff beam elements to virtually eliminate any chordwise warpage of the analytical model. Additional elements (with no mass) were located at the leading and trailing edges to obtain displacements around the perimeter of the model for use in the aeroelastic analysis. Natural frequencies, natural mode shapes, and generalized masses were calculated using EAL. Calculated natural frequencies are given in Table 1. Some of the corresponding calculated node lines are shown in Fig 11

A flutter analysis software system, known as FAST[6], was used to predict the aeroelastic
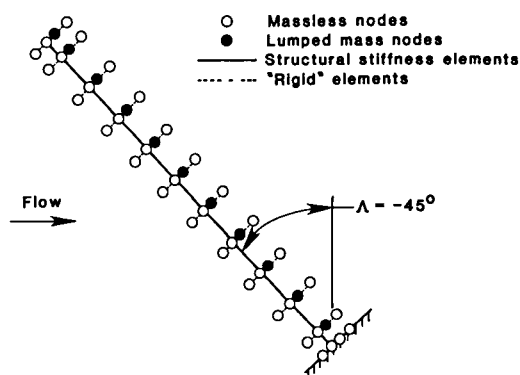
4

Fig. 9.- Finite element model of the experimental wing.

instabilities of the model. FAST calculates planar subsonic kernel function lifting-surface aerodynamics based on the natural mode shapes, natural frequencies, and generalized masses (as calculated through EAL) for the wing being analyzed. Four primary natural vibration modes (identified in Table 1, excluding first chordwise bending) were used in the present analysis. An aeroelastic instability solution is then completed by FAST with these calculated aerodynamics by the k method'. Divergence calculations are made by FAST provided the aerodynamics are calculated for a reduced frequency of zero.

Aeroelastic calculations were made for the various sweep angles by varying the sweep of the analytical lifting surface. In the experiment, the wing was pivoted to the various sweep angles about a point on the trailing edge of the wing at the wing root. Therefore, a small portion of the wing near the root constraint was not in the

(a) Bending stiffness
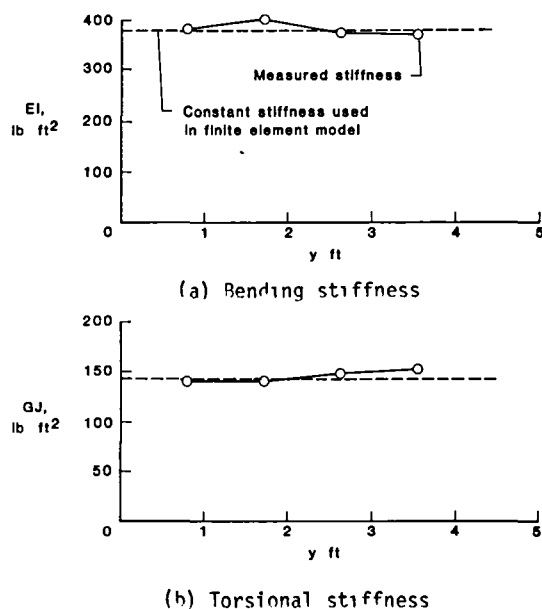

(b) Torsional stiffness

Fig. 10.- Measured stiffnesses.

flow (due to the splitter plate, see Fig. 4) in the forward-sweep positions. The planforms used in the analysis for the various sweep positions corresponded to the appropriate portion of the experimental model exposed to the flow. A small gap between the splitter plate and the wing surface allowed the structure to be identical in all the sweep angles Therefore, the simulated structure of the model was identical for all of the sweep configurations. In addition, the structure was considered to remain the same for the two wing tip shapes. The physical change in the wing tip shape had no significant affect on the structural properties The wing tips were modeled analytically by changing the planform geometry to account for the aerodynamic changes induced by the wing tip shapes. The analytical wing tip shapes correspond to the geometry shown in Fig. 5 without the airfoil-shaped body-of-revolution fairings on the extreme tip.

(a) First bending
$f_a = 5.4$ Hz

(b) Second bending
$f_a = 33.6$ Hz

(c) First torsion
$f_a = 62.5$ Hz

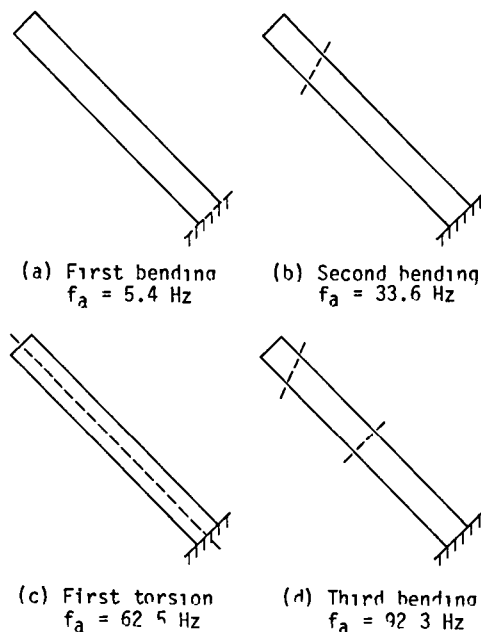(d) Third bending
$f_a = 92.3$ Hz

Fig. 11.- Calculated node lines and natural frequencies.

RESULTS AND DISCUSSION

Subcritical Response Techniques

Divergence predictions were made during the wind-tunnel test using the improved static Southwell method and the divergence index method. Typical basic data used in the divergence predictions is shown in Fig. 6 for the rectangular tip model. Fig. 7 and Fig. 8, respectively, show typical improved Southwell method and divergence index method divergence prediction measurements made during the wind-tunnel test. Although these methods generally provided linear data from which to make divergence predictions, Fig. 7b shows the type of experimental scatter to which such methods may be susceptible. In this particular case, $\Lambda = -60°$, the higher dynamic pressure data was given greater weight by ignoring the three

lowest dynamic pressure data points shown in Fig. 7b. The divergence index method, Fig 8b, was similarly affected. In this case, the first three data points also were ignored and the fourth dynamic pressure data point was used as the reference condition

An indication of the possible accuracy of these two prediction methods is shown in Figure 12a-e. These plots show how the predicted divergence dynamic pressure varied as the experimental dynamic pressure was increased. Both axes of the figure have been normalized by q_{ref} which is the divergence dynamic pressure predicted by the Southwell method after data had been obtained at the highest experimental dynamic pressure. In order not to damage the model, the dynamic pressure was not increased until divergence actually occurred. Based on the reference condition chosen, Fig 12 shows that for predictions made at a dynamic pressure within 35% of the final predicted divergence condition, the predictions are accurate within about ±10%. On the other hand, Fig. 12 also indicates the lack of extreme accuracy because of the experimental scatter exhibited by this model.

Test Results

Divergence measurements were made during the TDT wind-tunnel test at M = 0.4 for sweep angles of 0°, -15°, -30°, -45°, and -60° with the rectangular tip shape   A tip parallel to the flow was tested only in the   Λ = -45° position.   The experimental results obtained with the Southwell method are shown in Fig. 13. These results show the dramatic decrease in divergence dynamic pressure that occurred even at small forward sweep angles compared to the unswept wing and that the most critical configuration was at Λ = -45°.

The effect of the two tip shapes tested is also shown in Fig. 13. The tip parallel to the flow increased the divergence dynamic pressure by 14 percent compared to the rectangular tip at Λ = -45°.   Tip effects similar to these have been documented previously for much lower aspect ratio wings[8].   These two tips are identical in the unswept position, so the effect of the tip may be progressively less as the sweep angle is decreased from Λ = -45° to Λ = 0°.

Analytical and Experimental Results

The FAST aeroelastic software system was used to calculate divergence conditions for the model in each sweep configuration   Four natural modes were used in the analysis.   These modes were the three lowest frequency vertical (flapwise) bending modes and the first torsion mode (Fig. 11). Analysis also was made for the parallel tip shape in the Λ = -45° configuration   The tip shape was modeled in the analysis by adjusting the planform geometry so that the tip was either rectangular with respect to the wing planform or parallel with the free-stream flow direction.   The correlation between experiment and analysis at M = 0.4 can been seen in Fig. 13.   The analysis was significantly conservative at all forward sweep
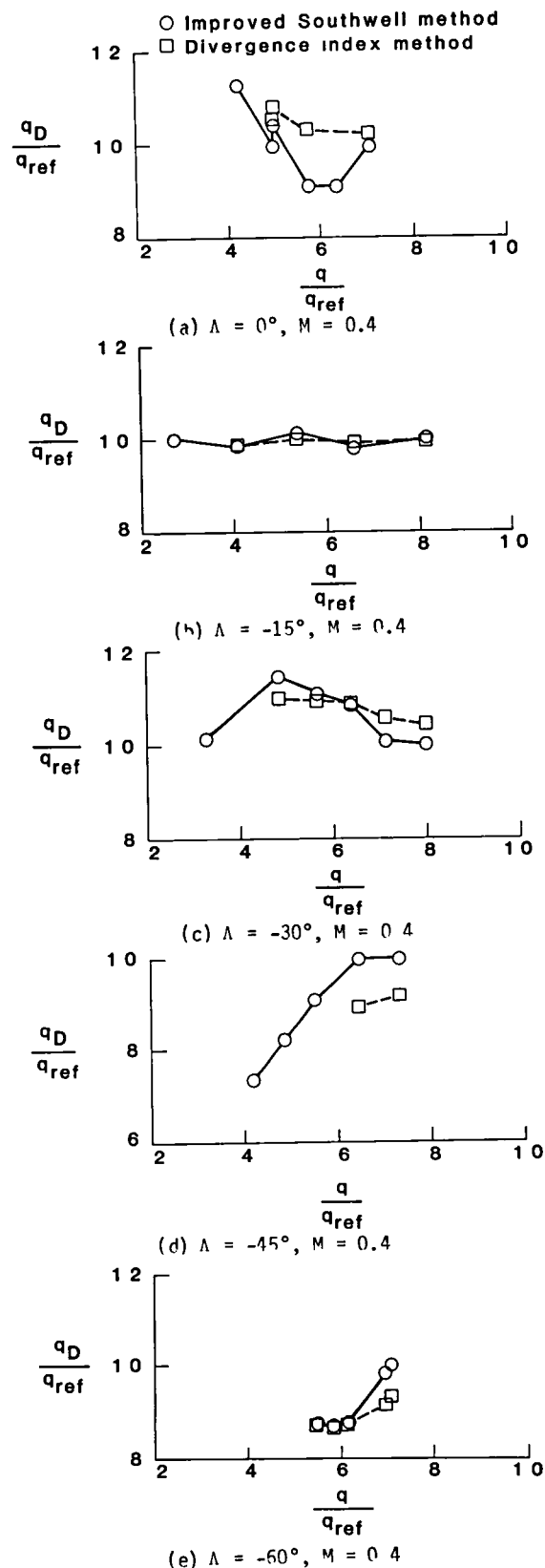

Fig. 12.- Variation of predicted divergence dynamic pressure as divergence is approached.
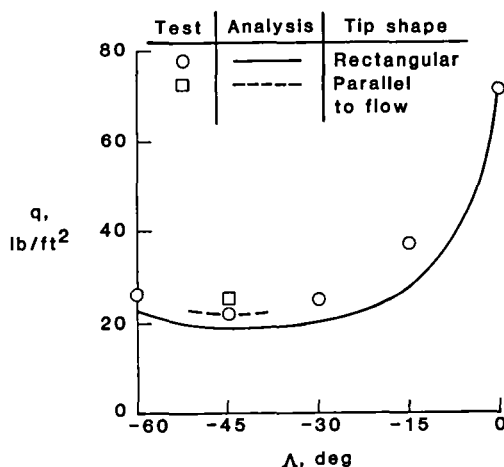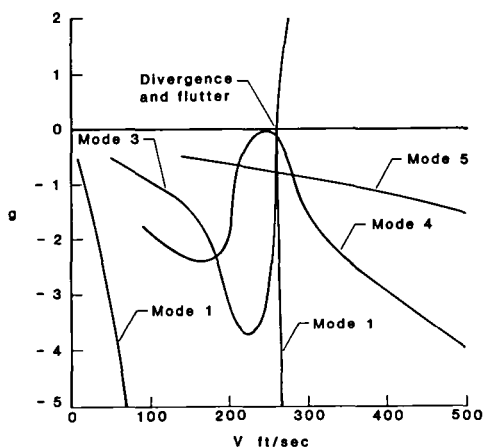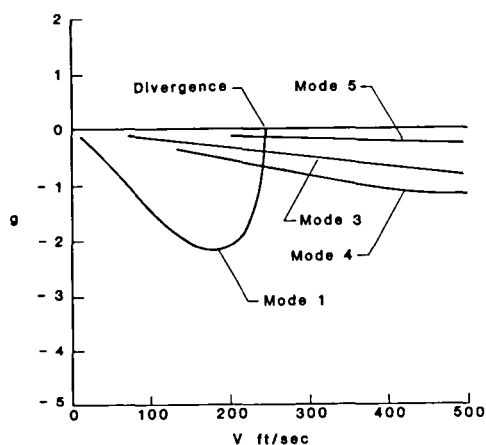
Fig. 13.- Divergence boundaries for both tip
models compared with calculated
boundaries.

(a) Λ = 0°, M = 0.5, ρ = 0.00207 sluos/ft³

(b) Λ = -45°, M = 0 5, ρ = 0.00062 sluos/ft³

Fig. 14 - Results of the aeroelastic analysis
near matched point conditions

angles. At Λ = -45°, the analysis was 14 percent conservative. In the unswept position, analysis matched the experimental results. The effect of the two tip shapes tested at Λ = -45° was predicted accurately by analysis. Typical calculated plots of velocity-versus-incremental damping are presented in Fig. 14a-b. Divergence was the critical instability at all sweep angles, although flutter was analytically predicted to occur at nearly the same dynamic pressure as divergence at Λ = 0° (Fig. 14a). This predicted flutter condition is primarily a coupling of the second vertical (flapwise) bending mode and the first torsion mode. Similar flutter results have been shown to occur in other forward-swept wing experiments (see ref. 4). In some instances, flutter is actually the critical instability at small forward sweep angles (-15° < Λ < 0°). This was not the case for the high-aspect ratio wing tested in this experiment. For this model, as the sweep angle was decreased, the flutter condition rapidly moved to higher velocities (higher dynamic pressures). Fig. 14b shows clearly that divergence is the predicted instability at Λ = -45°.

Analysis was conducted at M = 0.3, 0.5, and 0 6 to determine the Mach number effect on divergence. The analytical divergence results are shown in Fig. 15. These results indicate that the divergence dynamic pressure decreases with increasing Mach number. The slope of this trend is very small at Λ = -45°, but increases as the sweep angle is moved away from the Λ = -45° position.
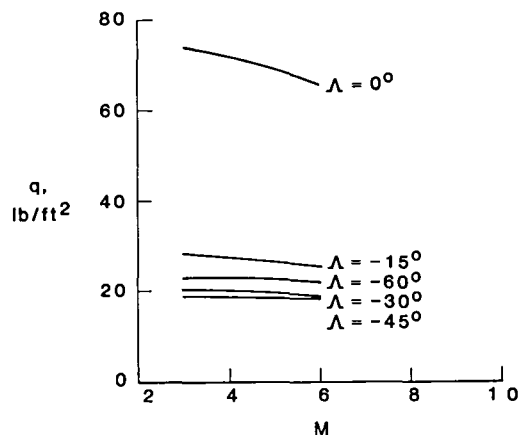

Fig 15.- Calculated effect of Mach number on
divergence for various sweep angles

CONCLUDING REMARKS

A study of static aeroelastic divergence has been conducted for a high-aspect ratio, forward-swept wing model. Divergence characteristics were determined experimentally and analytically at sweep angles of 0°, -15°, -30°, -45°, and -60°. A rectangular tip shape was tested for all sweep angles. In addition, for Λ = -45°, a tip parallel to the flow was tested.

The experimental divergence conditions were predicted using subcritical response test techniques. The divergence dynamic pressure predictions improved as the divergence condition was neared.

The wing tip shape had a significant effect on the divergence phenomenon. For Λ = -45°, a wing tip parallel to the flow increased the divergence dynamic pressure by 14 percent compared to a rectangular wing tip.

The analytical predictions using subsonic lifting surface theory were significantly conservative. At Λ = -45°, the analysis predicted a divergence dynamic pressure 14 percent lower than the experimental value.

REFERENCES

1. Williams, R M.· Application of Circulation Control Rotor Technology to a Stopped Rotor Aircraft Design Vertica, Vol. 1, Pergamon Press, Great Britain, 1976.

2. White, S., and Kelley, H L   Flight Research Capabilities of the NASA/Army Rotor Systems Research Aircraft (RSRA), Paper No 72, 4th European Rotorcraft and Powered Lift Aircraft Forum, Stresa, Italy, September 13-15, 1978.

3. Reed, Wilmer H.. Aeroelasticity Matters· Some Reflections of Two Decades of Testing in the NASA Langley Transonic Dynamics Tunnel. NASA TM-83210, 1981.

4. Ricketts, Rodney H., and Doggett, Robert V., Jr. Wind-Tunnel Experiments on Divergence of Forward-Swept Wings. NASA TP-1685, 1980.

5 Whetstone, W. D.·   EISI-EAL Engineering Analysis Language Reference Manual. Engineering Information Systems, Inc., 1983.

6. Desmarais, Robert N., and Bennett, Robert M.· User's Guide for a Modular Flutter Analysis Software System (FAST Version 1.0). NASA TM-78720, 1978.

7. Desmarais, Robert N., and Bennett, Robert M   An Automated Procedure for Computing Flutter Eigenvalues. Journal of Aircraft, Vol. 11, No. 2, 1974.

8. Diederich, Franklin W., and Budiansky, Bernard   Divergence of Swept Wings. NACA TN-1680, 1948.

1 Report No NASA TM-87682	2 Government Accession No	3 Recipient's Catalog No
4 Title and Subtitle DIVERGENCE STUDY OF A HIGH-ASPECT RATIO, FORWARD-SWEPT WING		5 Report Date June 1986
		6 Performing Organization Code 505-63-21-02
7 Author(s) Stanley R. Cole		8 Performing Organization Report No
9 Performing Organization Name and Address NASA Langley Research Center Hampton, VA 23665-5225		10 Work Unit No
		11 Contract or Grant No
12 Sponsoring Agency Name and Address National Aeronautics and Space Administration Washington, DC 20546		13 Type of Report and Period Covered Technical Memorandum
		14 Sponsoring Agency Code

15 Supplementary Notes

16 Abstract

An experimental wind-tunnel study to determine the divergence characteristics of a high-aspect ratio, forward-swept wing has been conducted in the NASA Langley Research Center (LaRC) Transonic Dynamics Tunnel (TDT). The rectangular wing used for this study had a panel aspect ratio of 9.16 ($\Lambda = 0^0$) and the sweep angle could be set at $\Lambda = 0^0$, -15^0, -30^0, -45^0, or -60^0. A rectangular wing tip shape was tested at each of these sweep angles. In addition, a tip shape parallel to the freestream flow was tested for a wing sweep angle of $\Lambda = -45^0$. The root of the wing was cantilever mounted to the wall of the wind tunnel. Divergence conditions were measured at $M = 0.4$ for each sweep angle and tip configuration tested. Subcritical response techniques were used to extrapolate to the divergence conditions during the wind-tunnel test. The primary objective of this test was to obtain data which could be used to verify for this configuration the divergence prediction capability of an aeroelastic analysis code. Subsonic lifting surface theory (kernel function) aerodynamics are utilized by this particular code. The analytical predictions of divergence were found to be significantly conservative at all forward sweep angles. At $\Lambda = -45^0$, the analysis was 14 percent conservative. The effect of the two tip shapes on the divergence dynamic pressure was predicted accurately by the analysis. The divergence condition for the tip shape parallel to the flow occurred at a dynamic pressure 14 percent higher than the divergence condition with a rectangular tip shape.

17 Key Words (Suggested by Authors(s)) Divergence High-Aspect Ratio Forward sweep Subcritical response techniques Aeroelasticity	18 Distribution Statement Unclassified - Unlimited Subject Category - 05		
19 Security Classif (of this report) Unclassified	20 Security Classif (of this page) Unclassified	21 No of Pages 9	22 Price A02

End of Document